nature energy

Article

https://doi.org/10.1038/s41560-023-01348-y

A contact-electro-catalytic cathode recycling method for spent lithium-ion batteries

Received: 28 September 2022

Accepted: 2 August 2023

Published online: 07 September 2023

Check for updates

Huifan Li[1,2], Andy Berbille[1,3], Xin Zhao[1], Ziming Wang[1,3], Wei Tang[1,3] ✉ & Zhong Lin Wang[1,3,4] ✉

With the global trend towards carbon neutrality, the demand for lithium-ion batteries (LIBs) is continuously increasing. However, current recycling methods for spent LIBs need urgent improvement in terms of eco-friendliness, cost and efficiency. Here we propose a mechano-catalytic method, dubbed contact-electro-catalysis, utilizing radicals generated by contact electrification to promote the metal leaching under the ultrasonic wave. We also use SiO_2 as a recyclable catalyst in the process. For lithium cobalt (III) oxide batteries, the leaching efficiency reached 100% for lithium and 92.19% for cobalt at 90 °C within 6 hours. For ternary lithium batteries, the leaching efficiencies of lithium, nickel, manganese and cobalt reached 94.56%, 96.62%, 96.54% and 98.39% at 70 °C, respectively, within 6 hours. We anticipate that this method can provide a green, high efficiency and economic approach for LIB recycling, meeting the exponentially growing demand for LIB productions.

Lithium-ion batteries (LIBs), widely used in various electronic devices and grid-scale energy storage, have become an important actor of our personal activities and the energy industry. Amid the rapidly growing adoption of portable electronics in communications, transportation and electricity, the demand for LIBs continues to grow. It is predicted that the amount of the spent LIBs will exceed 11 million tons worldwide by 2030 (ref. 1), representing an enormous source of pollution that could greatly threaten the environment and public health[2]. Meanwhile, the constantly increasing demand for LIBs translates into a growing demand for lithium and cobalt[3]. The International Energy Agency reports that the global battery and minerals supply chains need to expand tenfold by 2030, for example, 50 more lithium mines, 60 more nickel mines and 17 more cobalt mines need to be built[4]. On the other hand, the contents of lithium and cobalt in LIB cathodes are as high as 15 and 7 wt%, respectively, much higher than those in mined ores and saline[5,6]. Therefore, recycling metal elements in the cathodes of waste LIBs are of great environmental, social and economic importance[7].

At present, LIB recycling mainly consists of three steps: pretreatment, metal extraction and metal separation. Pretreatment normally refers to disassembly, shredding and comminution. To facilitate LIB recycling, battery manufacturers are required to consider rapid, efficient and safe disassembly processes in battery assembly design[8,9]. In the research and development of the metal-extraction step of the recycling process, the usual approach includes pyrometallurgy processes, hydrometallurgical recycling methods and direct recycling methods[10]. Although pyrometallurgy is widely used in the industry for its simplicity (without the need for pretreatment) and high efficiency, it also presents disadvantages, including the need of extreme temperatures (1,400 °C or higher) and the generation of toxic gases, leading to high infrastructure investments[11]. Direct recycling methods are beneficial because it allows batteries to be used directly after regeneration, avoiding a

[1]CAS Center for Excellence in Nanoscience, Beijing Institute of Nanoenergy and Nanosystems, Chinese Academy of Sciences, Beijing, China. [2]Center on Nanoenergy Research, School of Physical Science and Technology, Guangxi University, Nanning, China. [3]School of Nanoscience and Technology, University of Chinese Academy of Sciences, Beijing, China. [4]Yonsei Frontier Lab, Yonsei University, Seoul, Republic of Korea. ✉e-mail: tangwei@binn.cas.cn; zhong.wang@mse.gatech.edu

https://doi.org/10.1038/s41560-023-01348-y

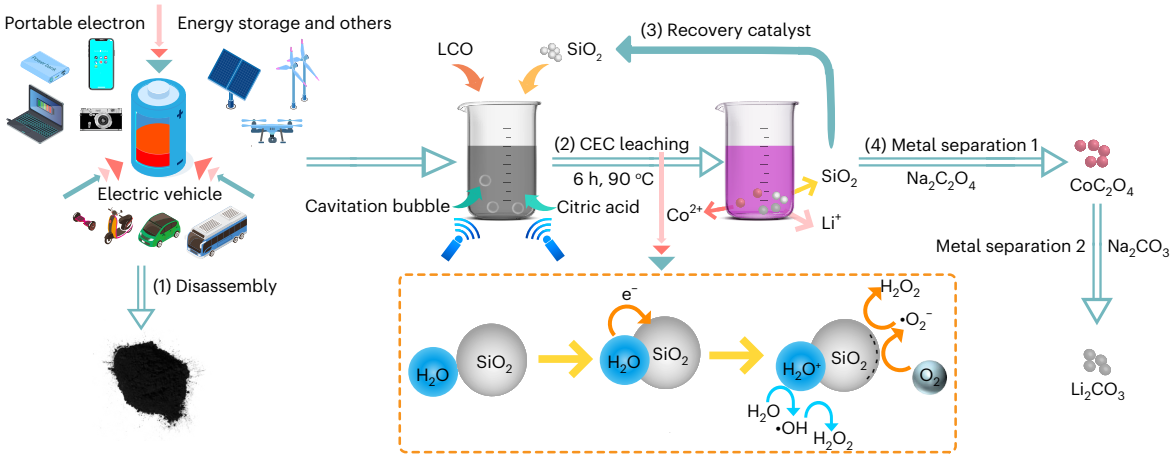

Fig. 1 | Flow chart of lithium battery recovery by CEC leaching. The spent lithium batteries are manually disassembled to obtain the electrode powder. Then the powder and SiO_2 catalyst are put into citric acid solution under ultrasonic conditions. After reaction, the catalyst and the leaching solution are separated by centrifugation. The obtained catalyst is used for the next-round leaching reaction, and the targeted metal ions in the leaching solution are separated by precipitation methods.

lengthy and expensive purification step. However, this process requires a rigorous sorting/pretreatment process, a clear assessment of the charging state and composition of batteries (to consider losses of lithium caused by the thickening of the solid electrolyte interface) and consistent purification, making it an inflexible technology[11,12]. Hydrometallurgical process is one of the most viable options, owing to its high metal-leaching rate and the satisfactory purity of the recovered product[13]. However, techniques employing hydrochloric acid (HCl)[14], phosphoric acid (H_3PO_4) (ref. 15) and other mineral acid[16] pose dangers to both workers and the environment, primarily because of harmful by-products (such as Cl_2, sulfur oxides and nitrogen oxides)[17]. Therefore, organic acids, such as succinic acid[18], citric acid[19] and malic acid[20], are now considered as promising alternatives. Nevertheless, organic acids also face their own set of challenges[17]. For example, additional reducing agents, such as hydrogen peroxide (H_2O_2), glucose or others, are required to accelerate the process, which, according to the classic '4H principle'[21], lowers economic returns. Recently, a deep eutectic solvent that acts as an effective leaching and reducing agent has been reported, but this process requires long reaction time (>24 h), high reaction temperature (>135 °C) and supplementary electrochemical processes to recycle the solvent[22].

Recently, the concept of contact-electro-catalysis (CEC) has been proposed, utilizing the electron transfer during liquid–solid contact electrification to generate free radicals to catalyse chemical reactions[23]. For example, Wang et al. utilized the formation of hydroxyl radical to degrade methyl orange[23] and Zare et al. demonstrated the generation of H_2O_2 by flowing water in glass microchannel[24]. Here we propose an approach by employing CEC to replace traditional reducing agents in the organic acid-leaching process. Specifically, in CEC, we provoke continuous solid–liquid contact and separation through the cavitation bubbles under ultrasound, thus leading to constant generation of reactive oxygen species through contact electrification. SiO_2 serves as the catalyst, which is recyclable. It is found that for the lithium cobalt (III) oxide (LCO), the leaching efficiency of lithium can reach 100% and that of cobalt is 92.19% at 90 °C. For the lithium nickel manganese cobalt oxide (NMC), the leaching efficiencies of Li, Ni, Mn and Co are found to be 94.56%, 96.62%, 96.54% and 98.39% at 70 °C, respectively. Because the characteristic of CEC involves recyclable catalysts (pristine dielectric materials) and mechanical-activated reaction region (stereoscopic), we anticipate that this method can provide a green, high efficiency and economical approach for LIB recycling, meeting the exponentially growing demand for LIB production.

The overall recycling processes

The whole recycling process is depicted in Fig. 1a. We first separated LCO from LIBs (as depicted in Supplementary Figs. 1 and 2 and Supplementary Table 1). Then metals are extracted by CEC leaching. In this step, we mix LCO and citric acid together, add SiO_2 as the catalyst and apply ultrasound as the source of mechanical energy. After 6 hours of reaction, the solution appears a pink colour, indicating the successful leaching of metals contained in the cathode material. The metals are then separated by successive precipitation, and the catalyst (SiO_2) is recycled. During the CEC-leaching process, according to previous literature[23], we proposed the CEC-leaching process as follows (Fig. 1): the ultrasonic wave causes the growth and collapse of cavitation bubbles, resulting in frequent contact electrification at the interface of SiO_2 and water. Thus, electrons are transferred from deionized (DI) water to the SiO_2 surface[25,26]. This process produces water radical cations that react with a water molecule (equation (1)) to form a hydroxyl radical and a hydronium ion[27]. During the collapse of the cavitation bubble, the oxygen present in the bubbles reacts with electrons on the surface of SiO_2, forming superoxide anions, as described by equation (2). Electrons, superoxide and hydroxyl radicals could all potentially participate in the leaching process. Finally, the precipitation method is performed to separate the mixture of lithium and cobalt ions in solution. $Na_2C_2O_4$ and Na_2CO_3 are added successively to react with Co^{2+} and Li^+ to form CoC_2O_4 and Li_2CO_3, precursors of LCO synthesis. It is worth noting that SiO_2 used for the whole process can be simply recycled by filtration method.

$$H_2O^+ + H_2O \rightarrow \cdot OH + H_3O^+ \quad (1)$$

$$e^-(SiO_2) + O_2 \rightarrow \cdot O_2^- + SiO_2 \quad (2)$$

where $e^-(SiO_2)$ represents the electron on SiO_2 surface.

Characterization of metal extractions by CEC-leaching process

We conducted investigations on different factors to optimize the CEC-leaching process. Figure 2a illustrates the impact of various dielectric materials on leaching efficiency. It is found that SiO_2 shows the best performance compared with PTFE (polytetrafluoroethylene), AlN (aluminium nitride) and POM (polyoxymethylene) due to the higher radical content under high temperature. Then we analyse the correlation between the quantity of SiO_2 and the leaching efficiency, as depicted in Fig. 2b. While the leaching efficiency increases from 0 to 80 mg, it

https://doi.org/10.1038/s41560-023-01348-y

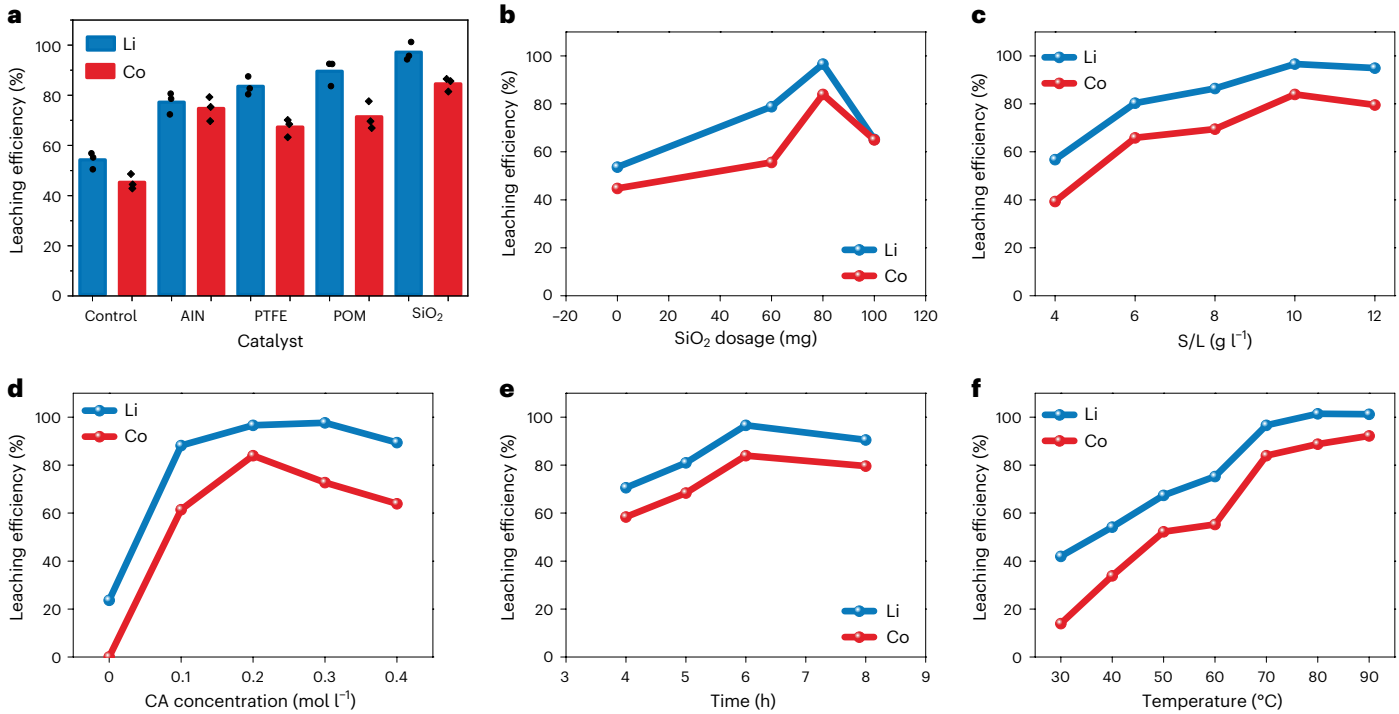

Fig. 2 | Metal extraction by CEC leaching. a–f, Influences of the choice of dielectric materials at 70 °C (**a**), SiO_2 dosage at 70 °C (**b**), S/L ratio at 70 °C (**c**), citric acid (CA) concentration at 70 °C (**d**), leaching time at 70 °C (**e**) and reaction temperature on the leaching efficiency of Li and Co for LCO batteries (**f**). Data are presented as mean values of three replicate data. The black diamond symbols correspond to the leaching efficiency of individual samples.

drops obviously between 80 and 100 mg. Indeed, an excessive amount of catalyst may induce the ultrasound waves to scatter, resulting in a reduction in efficiency[28,29]. And Supplementary Fig. 3 shows the effect of particle size of SiO_2 on leaching efficiency. Figure 2c shows the leaching efficiency increases as the solid/liquid ratio (S/L), namely the weight of LCO over the volume of the solution, until it saturates. Subsequently, we examine the influence of citric acid (CA) concentrations, as illustrated in Fig. 2d. We observed that the leaching efficiency of lithium increases when the concentration increases from 0.1 to 0.3 mol l^{-1}, owing to the promotion of the reaction between protons and lithium ions, until the lithium is released from the LCO framework[7]. While that of cobalt decreases to 73.12%, the increase of CA concentration results in higher ion concentration in the solution, thus impeding charge transfer between the water and the particle interface, due to the screening effect[30]. Therefore, there is a trade-off. The leaching time is shown in Fig. 2e, indicating that the leaching efficiency tends to be saturated when the time is over 6 h. Finally, Fig. 2f illustrates the influence of temperature. Because the metal-leaching process is endothermic, higher reaction temperatures create thermodynamically favourable conditions for leaching[31], so the highest efficiency is observed at 90 °C. In light of those results, we selected SiO_2 as the catalyst, and the CA concentration is 0.2 mol l^{-1}, SiO_2 dosage is 80 mg, the S/L is 10 g l^{-1} and the reaction temperature and time is set at 90 °C and 6 h. On this condition, the Li and Co leaching efficiency recorded as 100% efficiency for Li and 92.19% for Co. Moreover, we test the recycling performance of CEC leaching on NMC, as shown in Supplementary Fig. 4. The leaching efficiencies for Li, Ni, Mn and Co are achieved at 94.56%, 96.62% and 96.54%, respectively, demonstrating the excellent recycling ability of the CEC-leaching process for a ternary lithium battery.

Mechanism investigations of the CEC-leaching process

Afterwards, we investigate the mechanism of the CEC leaching. Figure 3a shows the trapping experiments. The leaching efficiency of Co^{2+} after 1 h obviously varied after different trapping agents were added. Specifically, when $AgNO_3$ is added into the solution, the leaching efficiency is drastically lowered, indicating that electrons are important active species in the leaching process, which implies CEC can generate electrons capable of participating in the reduction of Co^{3+} to Co^{2+}, as shown in equation (3). Moreover, the addition of tert-butanol as a scavenger for hydroxyl radicals also resulted in obviously lower leaching efficiency, indicating the important role of hydroxyl radicals in CEC leaching. This may be attributed to that hydroxyl radicals favour the break of the Co–O bond, which helps Co dissociate from the LCO skeleton. As a result, the Co cations are more readily available to interact with electrons at the surface of SiO_2, leading to an improved Co recovery efficiency. Additionally, capturing superoxide radicals with p-benzoquinone also dampens the leaching efficiency. We speculate that on one hand, $\cdot O_2^-$ could contribute directly to the reduction of metal, as shown in equation (4)[32,33]. On the other hand, $\cdot O_2^-$ can obtain protons to produce H_2O_2 under acidic conditions, as depicted in equation (5)[34], so as to leach metals with hydrogen peroxide behaving as in the acid-leaching reaction (equation (6)). Moreover, to further confirm the generation of hydroxyl radicals and electrons, electron spin-resonance spectroscopy (ESR) has been employed. At first, to detect hydroxyl radicals, the spin-trapping reagent DMPO (5,5-dimethyl-1-pyrroline N-oxide) is utilized. As shown in Fig. 3b, after adding DMPO trapping agent under CEC reaction conditions, we can find the typical quadruplet peak of DMPO-OH (1:2:2:1), indicating that the catalytic process of CEC results in the production of hydroxyl radical. In addition, the presence of electrons in the reaction system was assessed by adding a spin-trapping reagent 2,2,6,6-tetramethylpiperidine-1-oxyl(TEMPO), as shown in Fig. 3c. An obvious triple ESR signal peak with an intensity of 1:1:1 decreased during the reaction time, indicating the generation of electrons, which participate in the valence-changing reaction of cobalt[35].

$$e^-(SiO_2) + LiCoO_2(III) + 4H^+ \rightarrow Li^+ + Co^{2+} + 2H_2O + SiO_2 \quad (3)$$

https://doi.org/10.1038/s41560-023-01348-y

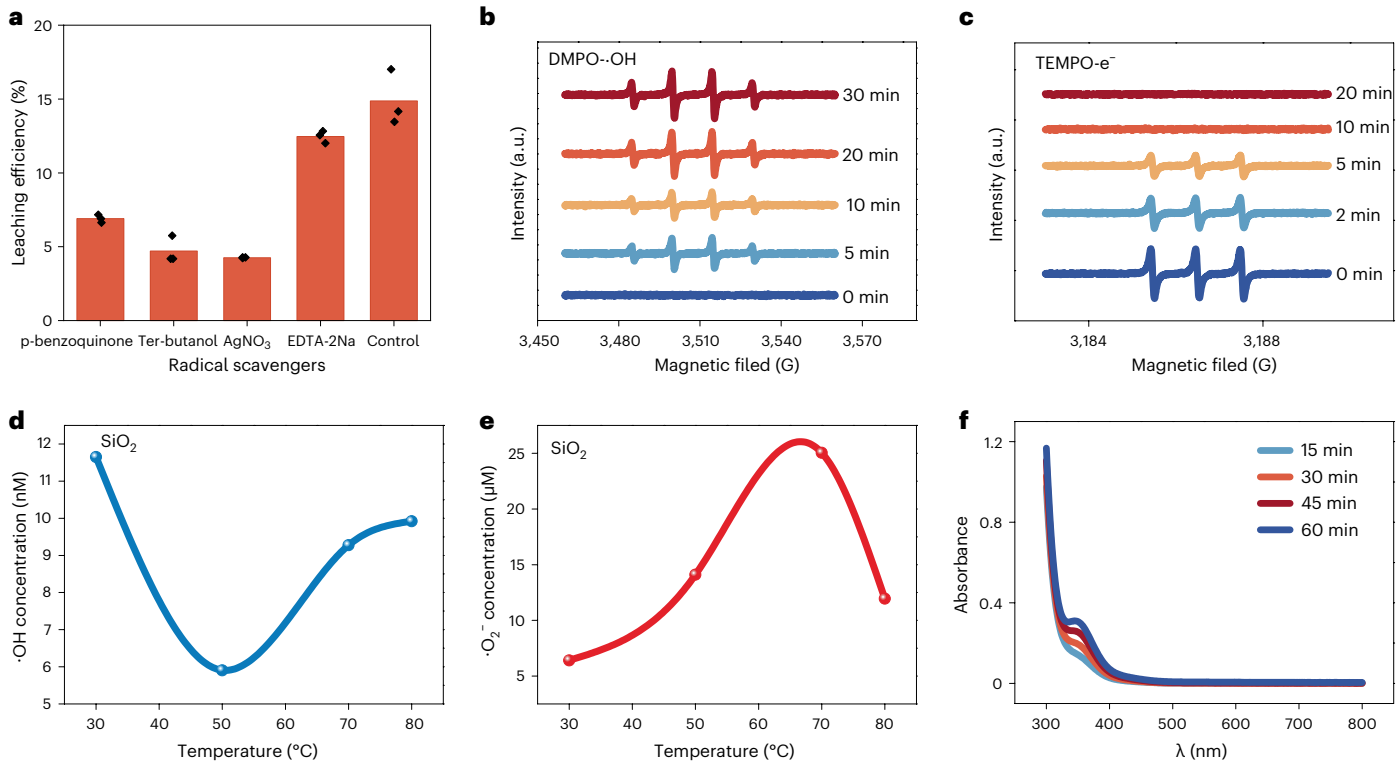

Fig. 3 | Investigations on the CEC-generated radicals for recycling. a, Leaching efficiency of Co for 1 h with various radical scavengers, including ter-butanol, p-benzoquinone, $AgNO_3$ and EDTA-2Na, which are respectively regarded as hydroxide radical, superoxide radical, electron and hole scavengers. The black diamond symbols correspond to the leaching efficiency of individual samples. **b**, ESR spectra of radical adducts signal trapped by DMPO. **c**, ESR spectra of radical adducts signal trapped by TEMPO for electrons. **d**, Fluorescence spectra of 2- hydroxy terephthalic acid (THA-OH) under ultrasonication in presence of SiO_2 microparticles. **e**, UV–vis spectra of NBT under ultrasonication in the presence of SiO_2 microparticles. **f**, UV–vis spectra with increasing reaction time by using ammonium molybdate spectrophotometry method. Data are presented as mean values of three replicate data.

$$O_2^- + LiCoO_2\,(III) + 4H^+ \rightarrow Li^+ + Co^{2+} + 2H_2O + O_2 \quad (4)$$

$$e^-\,(SiO_2) + \bullet O_2^- + 2H^+ \rightarrow H_2O_2 + SiO_2 \quad (5)$$

$$H_2O_2 + LiCoO_2\,(III) + 3H^+ \rightarrow Li^+ + Co^{2+} + 5/2H_2O + 3/4O_2 \quad (6)$$

Considering the effect of temperature on the acid-leaching process and on charge transfers in contact electrification, we measured the amount of ·OH and $\cdot O_2^-$ generated at different temperatures. First, we evaluated the concentration of hydroxyl radical generated in the CEC-leaching process by THA-OH fluorescent probe method. Figure 3d shows the change of ·OH concentration with temperature and control experiments exhibited in Supplementary Fig. 5a–e. The ability to form ·OH increases at 70 °C due to the enhancement of CE. As the temperature increases, the number of transferred electrons will increase[36] so that ·OH content increases with temperature[37]. Then we also tested the ability to generate ·OH of different dielectric materials at different temperatures (Supplementary Fig. 5f–k), which indicated that electronegative materials possess a higher capacity to generate hydroxyl radicals at suitable temperatures. On the other hand, to detect superoxide radicals, nitro blue tetrazolium (NBT) was employed[38] (Fig. 3e), and control experiments are shown in Supplementary Fig. 6a,b. It can be found that the content of superoxide free radicals increases gradually from 30 °C to 70 °C and decreases at 80 °C. The observed increase in superoxide free-radical generation from 30 °C to 70 °C may arise from the enhanced charge transfers as the temperature increases[37]. However, the dropping concentration of superoxide radicals at 80 °C could owe to the decreasing solubility of air in water as temperature increases[39], thus counterbalancing the benefits of enhanced charge transfers in this condition. As a result, the reactions presented in equations (4) and (5) are suppressed. Supplementary Fig. 6c–f displays the performance outcomes of alternative materials. More importantly, H_2O_2 is widely used in hydrometallurgy. And Zare et al. has reported that H_2O_2 can be spontaneously produced from the hydroxyl groups on the solid surface when water–solid contact occurred[24]. So we test the generation of H_2O_2 during the CEC-leaching process as shown in Fig. 3f. With the extension of reaction time, the intensity at 350 nm gradually increased, indicating the continuous generation of hydrogen peroxide. Furthermore, to evaluate the performance of contact electrification at the water–SiO_2 interface, we designed a single-electrode triboelectric nanogenerator (SE-TENG), made up of SiO_2 and electrode layers. Upon removing the SiO_2 and electrode from DI water, a potential difference is created between the electrode and the ground, thus causing electron flow detected by the electrometer[40,41]. Supplementary Fig. 7 demonstrates the amount of transferred charge to be approximately 1.41 nC, thereby confirming the occurrence of charge transfer during contact electrification.

Therefore, we summarize the mechanism of the CEC-leaching process. Ultrasonic conditions induce the generation and collapse of cavitation bubbles. Simultaneously, they produce a high-pressure microjet of water molecules that collide with SiO_2, thus causing electron transfer from water to SiO_2. The water radical cation will quickly react with a water molecule to form a hydroxyl radical and a hydronium, as shown in equation (1), and ·OH will break the Co–O bond and promote the reactions described by equations (3), (4) and (6). Electrons on the SiO_2 surface will reduce Co^{3+} to Co^{2+} (equation (1)) to realize the metal leaching. Oxygen in the cavitation bubbles can grab electrons from the SiO_2 surface, forming

https://doi.org/10.1038/s41560-023-01348-y

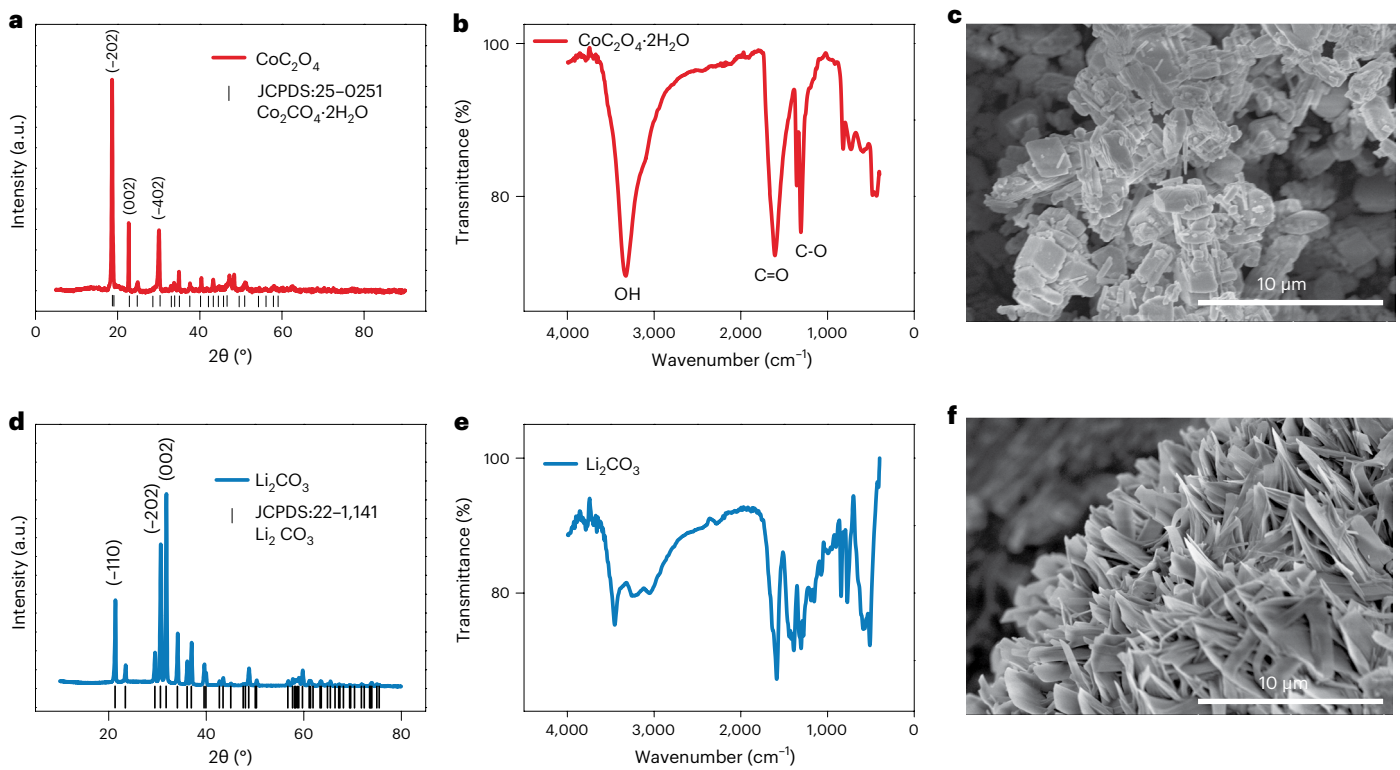

Fig. 4 | Characterization of precipitate from leaching solution after CEC treatment. a, XRD spectra of CoC_2O_4. **b**, FTIR spectra of CoC_2O_4. **c**, SEM image of CoC_2O_4. **d**, XRD spectra of Li_2CO_3. **e**, FTIR spectra of Li_2CO_3. **f**, SEM image of Li_2CO_3.

superoxide anions (equation (2)), and leaching metal from LCO can be described using the reaction equation from equations (4)–(6).

Precipitation after CEC leaching

After the leaching process, we obtain a leaching solution that contains a mixture of Li and Co ions that need to be separated and recovered from the solution for further use. Hence, we add $Na_2C_2O_4$ into the leaching solution and obtained the CoC_2O_4 pink precipitate. Figure 4a–c shows the properties of obtained CoC_2O_4. Figure 4a shows the X-ray diffraction (XRD) peaks are consistent with the standard card of CoC_2O_4 (PDF#25-0251), which indicates the formation of CoC_2O_4. Moreover, the Fourier-transformed infrared spectroscopy (FTIR) shows obvious characteristic peaks of CoC_2O_4 and confirms the same results as XRD. Notably, the peak at 1,605.84 cm^{-1} is assigned to asymmetric vibration of the C–O bond, and the closely spaced bands at 1,356.46 and 1,308.24 cm^{-1} are assigned to symmetric vibration of the C–O bond, illustrating the presence of bridged oxalates with all four oxygen atoms in coordination with the metal atom. Scanning electron microscopy (SEM) image shows the cobalt oxalate precipitate presents a lamellar structure[42]. After removing cobalt ions from the solution by precipitation method, saturated sodium carbonate was added to the lithium-rich solution to produce lithium carbonate precipitation. Figure 4d–f illustrates the XRD pattern, FTIR spectra and SEM image of the obtained Li_2CO_3. The XRD pattern of the Li precipitate corresponds to that of Li_2CO_3. Moreover, the peaks of the FTIR at 1,152.78 cm^{-1} attributed to the vibration of the symmetric C–O (ref. 43) and the band located at 1,388.75 cm^{-1} and 1,585.45 cm^{-1} assigned to antisymmetric stretching vibrations of the C–O bond of Li_2CO_3 (ref. 44) confirm the precipitate is Li_2CO_3.

Recyclability of the catalyst

Afterwards, we assessed the recyclability of the catalysts. We tried different methods to recover SiO_2 as shown in Fig. 5a. Method O, A and B are chemical treatment methods, employing aqua regia, HCl (50%) and NaOH (10%), respectively. It appears using these treatments is detrimental to the leaching efficiency and require two or three steps. If we do not recycle by chemical method but directly add the precipitation after the reaction to the next batch (Method C), the leaching efficiency is higher. And the leaching performance has no obvious decrease after recycling the powder five times, as seen in Fig. 5b. The infrared spectrum shows both pure silica and recycled silica present obvious antisymmetric stretching vibration peaks of Si–O–Si at 1,021.17 cm^{-1} and obvious characteristic absorption peaks of silica at 439.11 and 796.41 cm^{-1}, indicating no obvious changes of chemical structure. In addition, SEM imaging (Fig. 5d–f) shows the microspheres morphology of SiO_2 and recycled SiO_2. More importantly, we evaluated the economics of this process, as shown in Supplementary Note 1 and Supplementary Fig. 8[45]. The input cost is US$73.975 kg^{-1} spent $LiCoO_2$ powders, and the revenues are US$82.961 kg^{-1} spent $LiCoO_2$ powders, so this method has a profit of US$8.986 kg^{-1} spent $LiCoO_2$ powders, which is excellent, as shown in Supplementary Table 2, compared to other acid-leaching methods. Therefore, the proposed process for recycling spent LCO batteries appears promising at the current scale. And it produces a small amount of waste (such as wastewater and exhaust gas) throughout the recycling process.

Conclusions

Here we demonstrate the feasibility of leaching metals from LIB cathode materials using contact-electro-catalysis. The CEC-leaching efficiency of Li and Co reached 100% and 92.19% for LCO in 6 hours at 90 °C, respectively, whereas those of Li, Ni, Mn and Co for NMC attained 94.56%, 96.62%, 96.54%, and 98.39% at 70 °C, respectively. To further enhance the leaching efficiency, further work needs to be focused on improving the catalyst or the reaction solution. For example, we could consider using micro/nanoengineering to achieve a higher

https://doi.org/10.1038/s41560-023-01348-y

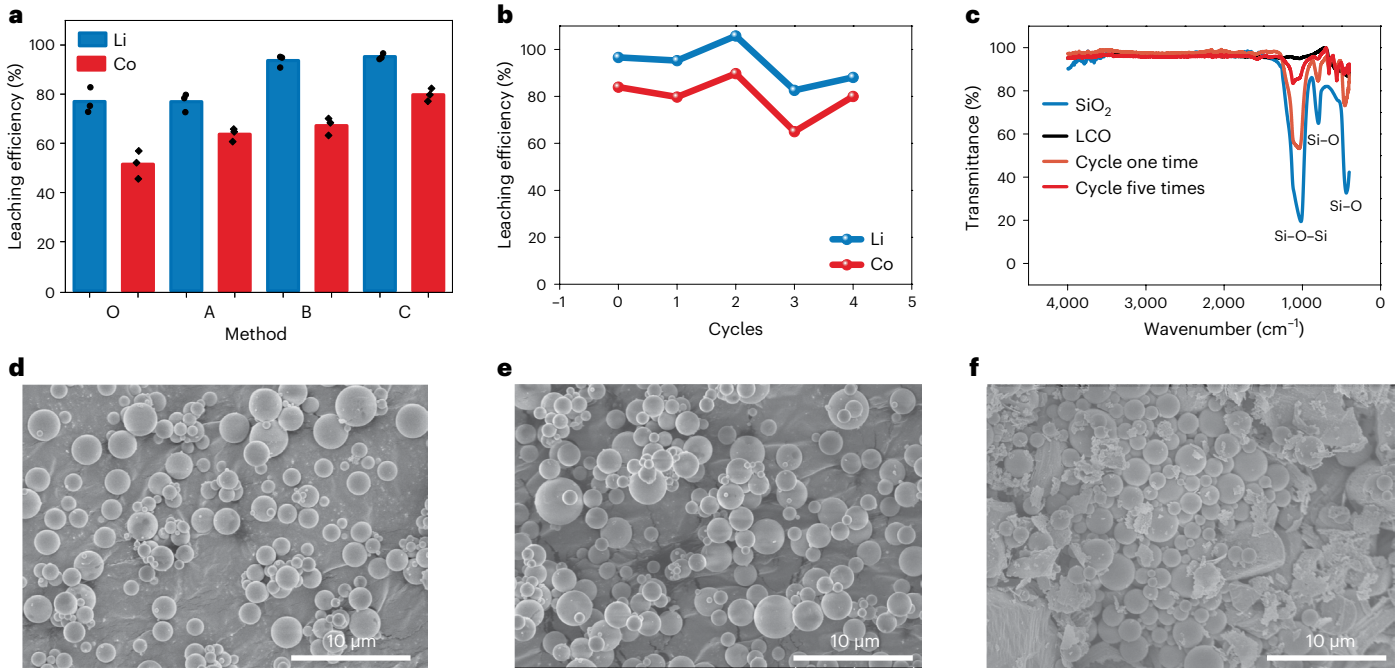

Fig. 5 | Recyclability demonstration of SiO_2 for CEC leaching. a, Leaching efficiency outcome for different methods employed to recycle the SiO_2 catalyst. The black diamond symbols correspond to the leaching efficiency of individual samples. O: using aqua regia, A: using 50% HCl, B: using 10% NaOH and C: no chemical reagents are applicable. **b**, Leaching efficiency of method C from one to five cycles. **c**, FTIR spectra of pure and recycled SiO_2. **d**, SEM image of SiO_2. **e**, SEM image of one cycled SiO_2. **f**, SEM image of five cycled SiO_2. Data are presented as mean values of three replicate data.

electrification ability for SiO_2, replacing SiO_2 by other dielectric materials with good temperature resistance or changing aqueous solution to organic solution for obtaining a higher reaction temperature. In this work, we also demonstrate that the compounds obtained by precipitation could be used as precursors for the synthesis of valuable products. Moreover, we verified that the SiO_2 as a catalyst can be successfully recycled. The CEC-leaching approach present in this work provides a promising solution to the sustainable recycling of LIBs with eco-friendliness, economic effectiveness and high efficiency. Meanwhile, we anticipate that it could also be noteable for recycling of noble metals such as silver and gold from electronic waste.

Methods

Chemical reagents

Two μm silicon dioxide (SiO_2, Aladdin, 99.95%), aluminium nitride (AlN, Macklin, 99.5%), fluorinated ethylene propylene (Dupont), Nylon-6,6 ($(C_{12}H_{22}N_2O_2)n$, Dupont), Polyoxymethylene (POM,$(CH_2O)n$, Dupont), p-phthalic acid (PTA, $C_8H_6O_4$, Macklin, 99%), p-Benzoquinone ($C_6H_4O_2$, Macklin, ≥99.5%), 2-hydroxybenzene-1,4-dioic acid ($C_8H_6O_5$, Macklin, ≥98.0%), Citric acid monohydrate ($C_8H_6O_7{\cdot}H_2O$, Sinopharm Chemical Reagent Co.), trisodium phosphate anhydrous (Na_3PO_4, Aladdin, 99.99%), ethylenediaminetetraacetic acid disodium salt ($C_{10}H_{14}N_2Na_2O_8{\cdot}2H_2O$, Aladdin, 99%), tert-butanol ($C_4H_{10}O$, Sinopharm Chemical Reagent Co., 98.0%), silver nitrate ($AgNO_3$, 99.8%, Sinopharm Chemical Reagent Co.), nitrotetrazolium blue chloride ($C_{40}H_{30}N_{10}O_6{\cdot}Cl_2$, Macklin, 98.0%), sodium carbonate (Na_2CO_3, Sinopharm Chemical Reagent Co.), sodium oxalate ($C_2Na_2O_4$, Sinopharm Chemical Reagent Co.) were used.

Pretreatment of spent LIBs

Discarded cell phone batteries were purchased from a Beijing, China, battery-recycling company. To recover the metal in spent lithium battery, it is necessary to pretreat the battery to get the electrode powder for recovery. The pretreatment mainly includes the following steps.

Discharging: to prevent spontaneous combustion and short circuiting during disassembly, the battery must be discharged first. It is immersed in a NaCl solution (10%, w/v) for 12 hours to complete the discharge, then rinsed four times with ultrapure water and dried for 12 hours in an oven at 60 °C. Disassembly: in the fume hood, the battery shell is removed with pliers and scissors. We then manually disassemble the aluminium film and separate the anode, cathode and diaphragm. Treatment of cathode film: the cathode film should be rolled out and cut into small pieces (2 cm × 2 cm), then placed into a crucible and heated in a muffle furnace at 500 °C for 30 minutes to remove cross-linking agents (PVDF and others). LCO is then stripped off the aluminium film. The material obtained is then ground to a powder with a mortar for the leaching experiment as illustrated in Supplementary Fig. 1.

Metal leaching using contact electrocatalyst

For the metal-recovery experiments, 80 mg of SiO_2 powder was added into a beaker containing 40 ml citric acid solution and then magnetically stirred at 550 r.p.m. for 1 h. 400 mg SLCO is added into the solution, and the beaker is placed into the ultrasonic bath (40 kHz, 120 W) for 6 h at 70 ± 3 °C. After ultrasonic treatment, the aliquots are centrifugated at 10,689 × *g* for 3 minutes. The concentrations of lithium and cobalt ions in the filtrate were measured by inductively coupled plasma optical emission spectrometer (ICP-OES).

The leaching efficiency (η) of LCO under different conditions was calculated by equation (7).

$$\eta = \frac{C_t V_t}{m\mathrm{w}\%} \times 100\% \tag{7}$$

where η is the leaching efficiency of metal (%), C_t is the metal concentration of Li or Co ion in the solution (mg l^{-1}), V_t is the volume of leaching solution (l); *m* is the mass of LCO powder; w% is the mass fraction of metals in the spent LCO powder.

Metal separation

Cobalt precipitation: 500 mg $Na_2C_2O_4$ was added to the leaching solution, stirred at room temperature for 30 minutes, then centrifuged to

obtain a sodium oxalate precipitate and a lithium solution. Lithium precipitation: the lithium-ion solution obtained in the previous step was reacted with saturated sodium carbonate and then stirred at 95 °C for 2 hours. The white lithium carbonate precipitate is then extracted from the solution by centrifugation.

SiO_2 recovery

We demonstrated it with three methods. In the first approach, the sonicated solution was centrifuged to obtain a mixture of residue and silica. Then, the residue was immersed into 30 ml 50% HCl and stirred at 70 °C for 1 hour. Next, the reaction solution was centrifuged to recover the silica, which was repeatedly cleaned with water and dried under vacuum for 5 h at 50 °C. In the second method, 10 wt% NaOH was used to dissolve SiO_2 and then precipitated with dilute hydrochloric acid to obtain SiO_2. The solution after the reaction was separated by centrifugation at 10,689 × *g* for 5 min to obtain precipitation and clearing. Then, the precipitate was added to 10% NaOH, heated at 90 °C for 1 hour, centrifuged, and the pH of obtained supernatant was adjusted to 7 with dilute HCl. Next, the precipitate was cleaned with water and dried under vacuum for 5 h at 50 °C. In the third method, the ultrasonic solution was centrifuged to obtain precipitation and clear liquid. The clear liquid is used for metal separation, and the precipitation is dried in a drying oven at 50 °C for 5 hours.

Free-radical test

The active species during the leaching reaction at 1 h were investigated by additionally dissolving 0.1 mM trapping agents including ter-butanol, p-benzoquinone, $AgNO_3$ and EDTA-2Na, which could capture ·OH, $\cdot O_2^-$, electron and hole, respectively. Then, 6,840 mg trisodium phosphate was added into 450 ml DI water and stirred to dissolve. Then, 2,991.6 mg terephthalic acid (THA) was added into the solution to obtain the buffered THA solution. 80 mg silica was added into 40 ml THA solution and sonicated for 1 h. Next, the fluorescence spectrum of the solution was tested under 312 nm excitation. NBT solution of 15 mg l^{-1} was prepared. 80 mg of silica was weighed and added to 40 ml NBT solution, and the mixture was sonicated for 30 minutes. The absorbance of the solution was measured with a UV–vis spectrophotometer.

Fabrication of SE-TENG

Before the experiment, the SiO_2 glass was rinsed with ethanol and dried in the oven. SiO_2 glass (6 × 5 cm^2) was carefully attached onto smooth copper tape and the glass was wrapped with waterproof tape. Smooth and clean PMMA plates (6 × 5 cm^2) were used as the substrates. The electric output of this SE-TENG device when repeatedly immersed in DI water stands for the intensity of contact electrification at the water–SiO_2 interface[46]. As the SiO_2 and electrode are pulled out of the solution, a potential difference is formed between the electrode and the ground, thus causing electron flow detected by the electrometer[40,41].

Characterization

Xpert3 powder XRD was used to characterize the structures of cobalt oxalate, lithium carbonate and silica powder before and after recycling. The scanning speed is set at 5° min^{-1}, and the scanning range is 5–90°. The morphology of cobalt oxalate, lithium carbonate and silica powder before and after recycling was obtained by SU8020 scanning electron microscopy. Lithium and cobalt ion concentrations were measured by Agilent ICP-OES 730. The absorption spectrum of NBT solution was analysed in an UV–vis spectrophotometer (Cary 3500 and Shimadzu UV-3600). The fluorescence spectra of THA and THA-OH are measured by full-function fluorescence spectrometer (FLS980-S2S2-stm). Electron spin-resonance spectrum (Bruker A300) recorded the changes of hydroxyl radicals and electrons over time.

Data availability

The data supporting the findings of this study are available within the paper and its Supplementary Information files. Source data are provided with this paper.

References

1. Lv, H. et al. Electric field driven de-lithiation: a strategy towards comprehensive and efficient recycling of electrode materials from spent lithium ion batteries. *Applied Catal. B* **283**, 119634 (2021).
2. Kang, D. H., Chen, M. & Ogunseitan, O. A. Potential environmental and human health impacts of rechargeable lithium batteries in electronic waste. *Environ. Sci. Technol.* **47**, 5495–5503 (2013).
3. Ciez, R. E. & Whitacre, J. F. Examining different recycling processes for lithium-ion batteries. *Nat. Sustain.* **2**, 148–156 (2019).
4. Global Supply Chains of EV Batteries (IEA, 2022); https://www.iea.org/reports/global-supply-chains-of-ev-batteries
5. Chernyaev, A. et al. The efficiency of scrap Cu and Al current collector materials as reductants in LIB waste leaching. *Hydrometallurgy* **203**, 105608 (2021).
6. Wang, S., Zhang, Z., Lu, Z. & Xu, Z. A novel method for screening deep eutectic solvent to recycle the cathode of Li-ion batteries. *Green Chem.* **22**, 4473–4482 (2020).
7. Yang, Y. et al. Selective recovery of lithium from spent lithium iron phosphate batteries: a sustainable process. *Green Chem.* **20**, 3121–3133 (2018).
8. Zeng, A. et al. Battery technology and recycling alone will not save the electric mobility transition from future cobalt shortages. *Nat. Commun.* **13**, 1341 (2022).
9. Or, T., Gourley, S. W. D., Kaliyappan, K., Yu, A. & Chen, Z. Recycling of mixed cathode lithium-ion batteries for electric vehicles: current status and future outlook. *Carbon Energy* **2**, 6–43 (2020).
10. Wang, Y. et al. Recent progress on the recycling technology of Li-ion batteries. *J. Energy Chem.* **55**, 391–419 (2021).
11. Raj, T. et al. Recycling of cathode material from spent lithium-ion batteries: challenges and future perspectives. *J. Hazard. Mater.* **429**, 128312 (2022).
12. Baum, Z. J., Bird, R. E., Yu, X. & Ma, J. Lithium-ion battery recycling—overview of techniques and trends. *ACS Energy Lett.* **7**, 712–719 (2022).
13. Garole, D. J. et al. Recycle, recover and repurpose strategy of spent Li-ion batteries and catalysts: current status and future opportunities. *ChemSusChem* **13**, 3079–3100 (2020).
14. Barik, S. P., Prabaharan, G. & Kumar, L. Leaching and separation of Co and Mn from electrode materials of spent lithium-ion batteries using hydrochloric acid: laboratory and pilot-scale study. *J. Clean. Prod.* **147**, 37–43 (2017).
15. Chen, X., Ma, H., Luo, C. & Zhou, T. Recovery of valuable metals from waste cathode materials of spent lithium-ion batteries using mild phosphoric acid. *J. Hazard. Mater.* **326**, 77–86 (2017).
16. Zhou, S. et al. Recycling of $LiCoO_2$ cathode material from spent lithium ion batteries by ultrasonic enhanced leaching and one-step regeneration. *J. Environ. Manage.* **277**, 111426 (2021).
17. Bai, Y. et al. Energy and environmental aspects in recycling lithium-ion batteries: concept of battery identity global passport. *Mater. Today* **41**, 304–315 (2020).
18. Li, L. et al. Succinic acid-based leaching system: a sustainable process for recovery of valuable metals from spent Li-ion batteries. *J. Power Sources* **282**, 544–551 (2015).
19. Gao, W. et al. Comprehensive evaluation on effective leaching of critical metals from spent lithium-ion batteries. *Waste Manage.* **75**, 477–485 (2018).
20. Li, L. et al. Recovery of metals from spent lithium-ion batteries with organic acids as leaching reagents and environmental assessment. *J. Power Sources* **233**, 180–189 (2013).

21. Fan, E. et al. Sustainable recycling technology for Li-ion batteries and beyond: challenges and future prospects. *Chem. Rev.* **120**, 7020–7063 (2020).
22. Tran, M. K., Rodrigues, M.-T. F., Kato, K., Babu, G. & Ajayan, P. M. Deep eutectic solvents for cathode recycling of Li-ion batteries. *Nat. Energy* **4**, 339–345 (2019).
23. Wang, Z. et al. Contact-electro-catalysis for the degradation of organic pollutants using pristine dielectric powders. *Nat. Commun.* **13**, 130 (2022).
24. Chen, B. et al. Water-solid contact electrification causes hydrogen peroxide production from hydroxyl radical recombination in sprayed microdroplets. *Proc. Natl Acad. Sci. USA* **119**, e2209056119 (2022).
25. Lin, S., Xu, L., Chi Wang, A. & Wang, Z. L. Quantifying electron-transfer in liquid–solid contact electrification and the formation of electric double-layer. *Nat. Commun.* **11**, 399 (2020).
26. Sun, M., Lu, Q., Wang, Z. L. & Huang, B. Understanding contact electrification at liquid–solid interfaces from surface electronic structure. *Nat. Commun.* **12**, 1752 (2021).
27. Lin, M.-F. et al. Imaging the short-lived hydroxyl-hydronium pair in ionized liquid water. *Science* **374**, 92–95 (2021).
28. Wang, J. et al. Sonocatalytic damage of bovine serum albumin (BSA) under ultrasonic irradiation by mixed TiO_2/SiO_2 powder. *J. Chem. Technol. Biotechnol.* **84**, 538–546 (2009).
29. Deveci, I. & Mercimek, B. Performance of SiO_2/Ag core/shell particles in sonocatalalytic degradation of rhodamine B. Ultrason. *Sonochem.* **51**, 197–205 (2019).
30. Zhan, F. et al. Electron transfer as a liquid droplet contacting a polymer surface. *ACS Nano.* **14**, 17565–17573 (2020).
31. Behera, S. S. & Parhi, P. K. Leaching kinetics study of neodymium from the scrap magnet using acetic acid. *Sep. Purif. Technol.* **160**, 59–66 (2016).
32. Hu, W. et al. Photocatalytic reduction of Cr(VI) using a wurtzite/natural sphalerite heterostructure: synergistic effects of exposed active facets, vacancies and a heterophase junction. *Appl. Surf. Sci.* **550**, 149267 (2021).
33. Liang, H. et al. 3-D hierarchical Ag/ZnO@CF for synergistically removing phenol and Cr(VI): heterogeneous vs homogeneous photocatalysis. *J. Colloid Interface Sci.* **558**, 85–94 (2020).
34. Nosaka, Y. & Nosaka, A. Y. Generation and detection of reactive oxygen species in photocatalysis. *Chem. Rev.* **117**, 11302–11336 (2017).
35. Xiao, R. et al. In situ fabrication of 1D CdS nanorod/2D Ti_3C_2 MXene nanosheet Schottky heterojunction toward enhanced photocatalytic hydrogen evolution. *Appl. Catal. B* **268**, 118382 (2020).
36. Xu, C. et al. Raising the working temperature of a triboelectric nanogenerator by quenching down electron thermionic emission in contact-electrification. *Adv. Mater.* **30**, e1803968 (2018).
37. Shen, F. et al. Influence of temperature difference on performance of solid–liquid triboelectric nanogenerators. *Nano Energy* **99**, 107431 (2022).
38. Huang, H. et al. Macroscopic polarization enhancement promoting photo- and piezoelectric-induced charge separation and molecular oxygen activation. *Angew. Chem. Int. Ed.* **56**, 11860–11864 (2017).
39. Geng, M. & Duan, Z. Prediction of oxygen solubility in pure water and brines up to high temperatures and pressures. *Geochim. Cosmochim. Acta* **74**, 5631–5640 (2010).
40. Rodrigues, C. et al. Emerging triboelectric nanogenerators for ocean wave energy harvesting: state of the art and future perspectives. *Energy Environ. Sci.* **13**, 2657–2683 (2020).
41. Lin, S., Chen, X. & Wang, Z. L. Contact electrification at the liquid–solid interface. *Chem. Rev.* **122**, 5209–5232 (2022).
42. Huang, Z. et al. Solution inheritance of $CoC_2O_4{\cdot}2H_2O$ rods to nanoparticle-assembled Co_3O_4 rods. *Colloids Surf. A* **490**, 307–317 (2016).
43. Qiu, X. et al. Enabling the sustainable recycling of $LiFePO_4$ from spent lithium-ion batteries. *Green Chem.* **24**, 2506–2515 (2022).
44. Cai, W., Chen, R., Yang, Y., Yi, M. & Xiang, L. Removal of SO_4^{2-} from Li_2CO_3 by recrystallization in Na_2CO_3 solution. *Crystals* **8**, 19 (2018).
45. Chen, X., Kang, D., Li, J., Zhou, T. & Ma, H. Gradient and facile extraction of valuable metals from spent lithium ion batteries for new cathode materials re-fabrication. *J. Hazard. Mater.* **389**, 121887 (2020).
46. Wang, K. et al. Hexadecane-containing sandwich structure based triboelectric nanogenerator with remarkable performance enhancement. *Nano Energy* **87**, 106198 (2021).

Acknowledgements

We appreciate C. Li, S. Shu and Y. Su for their assistance with collecting and organizing data. This research was supported by the National Key R&D Project from the Minister of Science and Technology (2021YFA1201601) and National Natural Science Foundation of China (grant number 52192610), Youth Innovation Promotion Association (W.T.) and CAS-TWAS President's Fellowship (A.B.).

Author contributions

W.T. and Z.L.W. conceived the idea and supervised the experiment. H.L., A.B. and X.Z. performed the experiments, H.L. and W.T. analysed the data. Z.W. assisted in data measurements. H.L., A.B. and W.T. prepared the manuscript. Z.L.W. revised the manuscript.

Competing interests

The authors declare no competing interests.

Additional information

Supplementary information The online version contains supplementary material available at https://doi.org/10.1038/s41560-023-01348-y.

Correspondence and requests for materials should be addressed to Wei Tang or Zhong Lin Wang.

Peer review information *Nature Energy* thanks Gavin Harper, Jia Li and the other, anonymous, reviewer(s) for their contribution to the peer review of this work.